Acta Acustica 2022, **6**, 52

https://doi.org/10.1051/aacus/2022048

Available online at:
https://acta-acustica.edpsciences.org

SCIENTIFIC ARTICLE OPEN ACCESS

Interaction between double nonspherical bubbles in compressible liquid under the coupling effect of ultrasound and electrostatic field

Jin-Jie Deng[1,2], Ming Yu[3,*], and Ri-Fu Yang[2]

[1] Department of Mechanical and Electrical Engineering, Yangjiang Polytechnic, Yangjiang 529500, China
[2] School of Physics, South China University of Technology, Guangzhou 510640, China
[3] Division of Quality Control, Yangtze Delta Region Institute of Tsinghua University, Jiaxing 314006, China

Received 1 July 2022, Accepted 27 October 2022

Abstract – A dynamic model for a double-bubble system in compressible liquid under the coupling effect of ultrasound and electrostatic field was developed here. In this study, we mainly discussed the effect of the interaction on the investigated bubble using the numerical solutions to the theoretic model. The variable parameters are the distance between bubble centers and the initial radius of the adjacent bubble. In addition, we applied approximate equations to analyse variations of the internal gas pressure and temperature of a bubble. We found that, the oscillation amplitude of a bubble with an adjacent bubble significantly reduces, compared to that of an isolated bubble.

Keywords: Ultrasound, Electrostatic field, Compressible liquid, Interaction double-bubble system

Nomenclature

θ_α	Azimuth of bubble α
θ_β	Azimuth of bubble β
S_α	Radius of bubble α
S_β	Radius of bubble β
$P_2(\cos\theta)$	Second-order Legendre function
$a_0(t)$	Spherical radius component of bubble α
$b_0(t)$	Spherical radius component of bubble β
$a_2(t)$	Coefficient of nonspherical radius component of bubble α
$b_2(t)$	Coefficient of nonspherical radius component of bubble β
ϵ	Small parameter
r_α	Distance from a point in the liquid to the center of bubble α
r_β	Distance from a point in the liquid to the center of bubble β
L	Distance between bubble centers
f_s	Electric stress
ϵ_0	Vacuum permittivity
ϵ_{rl}	Relative permittivity
E	Electric field strength in the liquid region
p_0	Static pressure of the liquid
p_v	Vapor pressure in the bubble
p_a	Acoustic pressure amplitude
σ	Surface tension at the liquid–gas interface
η	Viscosity of the liquid
γ	Adiabatic index
R_0	Initial bubble radius
R	Bubble radius
$\dot{R}$	Interface velocity
ω	Angular frequency of the acoustic wave

1 Introduction

As an efficient, environmentally-friendly and economical technology, the combination of an electric field with ultrasound has been widely used in laboratories and industrial fields in recent years. A study by Jung et al. [1] revealed that this combined treatment can be used to disintegrate waste activated sludge. After 60 min treatment time, the average particle size of the sludge decreased significantly more, compared to ultrasonic treatment alone. In addition, Yang et al. [2] used the ultrasound-synergized electric field extraction (UEE) to extract flavonoids from hemerocallis citrina baroni (a citron daylily). They found that the yield of flavonoids was 10% higher using UEE than conventional ultrasound extraction, and it was 18% higher than water bath extraction. A work by Yang et al. [3] reveals the mechanism how electric stress strengthens ultrasonic cavitation. However, many details of interactions between nonspherical bubbles are not known. In fact, when cavitation occurs in the liquid, it can generate a high number of cavitation

*Corresponding author: mingyufem@163.com

bubbles, instead of a single one. The interactions between these adjacent bubbles affect the oscillation of the individual bubbles significantly, which should be considered in the mathematic model. To describe the effect of an adjacent bubble on the cavitation of an investigated bubble, we need to develop a dynamic equation-set including the interaction between double bubbles.

Many researchers helped advance the theoretical model for two interacting bubbles. Li et al. [4], Pityuk et al. [5], and Wang et al. [6] provided three different mathematical models for two adjacent spherical bubbles in an ultrasonic field. In the study of CCl_4 sono-pyrolysis, Merouani et al. [7–9] used modified Keller-Miksis equations to analyze the thermal effect and the interaction between bubbles. Shima and Fujiwara [10] investigated the behavior of two spherical bubbles with different sizes near a solid wall and derived the motion equations for two bubbles. However, these models are unsuitable for two interacting nonspherical bubbles in the presence of an electric force. The variation of nonspherical radius components of bubbles cannot be obtained by simply modifying the models for spherical bubbles. Liang et al. [11] developed a dynamic model for two native nonspherical bubbles in an incompressible liquid. However, their derivation includes some important inaccuracies, which leads to incorrect mathematic equations. Furthermore, in the calculation of the total velocity potential near the interface of a bubble, they did not consider the perturbing velocity potential induced by the interaction between bubbles, which is an additional term of the total velocity potential. In addition, none of the above-mentioned studies considered the liquid's compressibility. If the liquid's compressibility is neglected in the numerical calculation, the maximum bubble- radius can easily be larger, and the minimum bubble-radius can be smaller, compared to the actual situation.

The present study aims to develop a dynamic model for nonspherical double-bubbles in a compressible liquid under the coupling effect of ultrasound and an electrostatic field. We used perturbation analysis, the sphere theorem, and the basic fluid-mechanics equations to derive the required model. We mainly analyze the effect of the interaction force on the investigated bubble using numerical solutions to the theoretical model. The variable parameters are: the distance between bubble centers, and the initial radius of the adjacent bubble. Furthermore, in the derivation, we offer an explanation why the effect of the liquid's compressibility cannot transfer from the area near the interface of one bubble to the one of another bubble, when the two bubbles are far apart from each other. Finally, we applied approximate equations to investigate temporal evolutions of the gas pressure and the temperature inside a bubble. These results can provide better insights into the oscillation mechanism of interacting nonspherical bubbles in a compressible liquid.

2 Model for double nonspherical bubbles

2.1 Interface equations for double bubbles

To describe a double-bubble system, we introduce a nonspherical function $S(\theta, t)$ with rotational symmetry, which is independent of the rotation angle ϕ. In spherical coordinates, the interface equations for double bubbles can be expressed as

$$S_\alpha = S_\alpha(\theta_\alpha, t) = a_0(t) + \epsilon a_2(t) P_2(\cos\theta_\alpha), \tag{1a}$$

$$S_\beta = S_\beta(\theta_\beta, t) = b_0(t) + \epsilon b_2(t) P_2(\cos\theta_\beta), \tag{1b}$$

where

$$P_2(\cos\theta_\alpha) = \frac{1}{2}\left(3\cos^2\theta_\alpha - 1\right), \tag{2a}$$

$$P_2(\cos\theta_\beta) = \frac{1}{2}\left(3\cos^2\theta_\beta - 1\right). \tag{2b}$$

The small parameter ϵ indicates that, for both bubbles, the nonspherical components are much smaller than the spherical components.

Figure 1 shows the sections of two nonspherical bubbles, which are elliptic. The distance L is set to hundreds of microns in this study, namely $L \gg S_\alpha + S_\beta$. The reason is that if two bubbles are too close, the coalescence of these two bubbles probably occurs. This is out of the scope of our discussion.

2.2 Total pressure-difference on the whole liquid region outside a bubble

The direction of the electric field is set to parallel to the line of bubble centers. For an insulating bubble, the expression for electric stress f_s [12, 13] is as follows:

$$f_s = \epsilon_0 \frac{(\epsilon_{rl} - 1)^2}{3} E^2 P_2(\cos\theta). \tag{3}$$

The electric stress f_s exerts on the bubble wall, stretching the bubble in the electric-field direction and compressing the bubble in the direction vertical to the electric field.

If a bubble undergoes adiabatic oscillation, the total pressure-difference on the whole liquid region outside this bubble can be written as

$$\begin{aligned}\Delta P &= \left(p_0 + \frac{2\sigma}{R_0} - p_v - \epsilon f_s\right)\left(\frac{R_0}{R}\right)^{3\gamma} + p_v - p_0 - \frac{2\sigma}{R} \\ &\quad - \frac{4\eta\dot{R}}{R} + \epsilon f_s - p_a\cos\omega t \\ &= \Delta P_1 + \epsilon f_e P_2(\cos\theta),\end{aligned} \tag{4}$$

where

$$\begin{aligned}\Delta P_1 &= \left(p_0 + \frac{2\sigma}{R_0} - p_v\right)\left(\frac{R_0}{R}\right)^{3\gamma} + p_v - p_0 - \frac{2\sigma}{R} - \frac{4\eta\dot{R}}{R} \\ &\quad - p_a\cos\omega t,\end{aligned} \tag{5}$$

$$f_e = \left[1 - \left(\frac{R_0}{R}\right)^{3\gamma}\right]\epsilon_0 \frac{(\epsilon_{rl} - 1)^2}{3} E^2. \tag{6}$$

For a nonspherical bubble, $R = a_0(t)$ or $b_0(t)$. To simplify the calculation, the bubble is considered to be

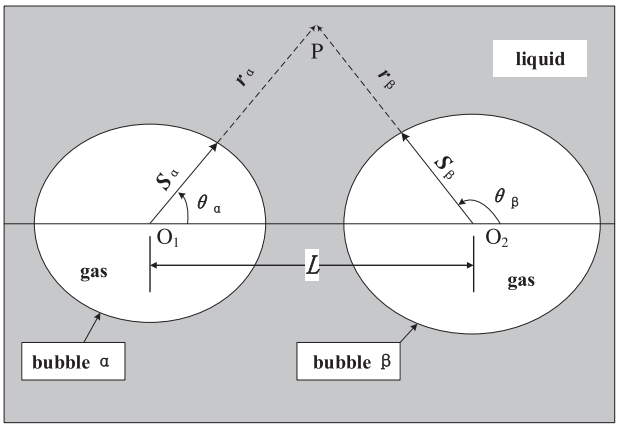

Figure 1. Sections of two nonspherical bubbles.

approximately spherical for the force analysis (Eqs. (6)–(8)). The rationality of this simplification is based on that the nonspherical term is much smaller than the spherical term for an elliptical bubble.

2.3 Derivation of the theoretical model

Let coordinates α be the spherical coordinates with the origin at the center of bubble α, and coordinates β be the spherical coordinates with the origin at the center of bubble β.

In coordinates α, the velocity potential of bubble α can be written as

$$\Phi_\alpha(r_\alpha,\theta_\alpha,t)=\Phi_{\alpha 0}(r_\alpha,t)+\epsilon\Phi_{\alpha 2}(r_\alpha,\theta_\alpha,t), \tag{7}$$

where

$$\Phi_{\alpha 0}(r_\alpha,t)\approx\frac{A_0(t)}{kr_\alpha}-\frac{\dot{A}_0(t)}{\omega}, \tag{8}$$

$$\Phi_{\alpha 2}(r_\alpha,\theta_\alpha,t)\approx P_2(\cos\theta_\alpha)\left[\frac{3A_2(t)}{k^3r_\alpha^3}+\frac{2A_2(t)}{kr_\alpha}+\frac{\dot{A}_2(t)}{\omega}\right]. \tag{9}$$

Here, $\Phi_{\alpha 0}$ (r_α, t) and $\Phi_{\alpha 2}(r_\alpha, \theta_\alpha, t)$ are the spherical component and the nonspherical component of the velocity potential of bubble α. k is the wave number, $k=\omega/c$, and c is the speed of sound in the liquid. $A_0(t)$ and $A_2(t)$ are two functions of time. The derivations of equations (10) and (11) (see Ref. [3]) are based on the assumption that ultrasonic wave propagates within an infinitely large liquid region. Hence, no standing wave occur in the liquid. This means that translational motions of bubbles cannot occur. Thus, the distance L can be considered constant.

In the dynamic model for bubble α, the interaction terms reflect the effects of bubble β on bubble α. The effect of the liquid's compressibility only occurs in the vicinity of the interface of a bubble, which cannot transfer to the liquid region far away from the interface of a bubble. Importantly, this effect cannot transfer to the vicinity of the interface of another bubble, when the two bubbles are far apart from each other. The reason for this is as follows: In the radial direction, as the distance from a bubble center to a point in the liquid increases, the fluid velocity decreases sharply. The effect of the liquid's compressibility is positively correlated with the fluid velocity. For a liquid region far away from the bubble interface, the fluid velocity is very small, the effect of the liquid's compressibility can therefore be neglected. Hence, in the derivation of the dynamic model for bubble α, the liquid's compressibility needs not to be considered when calculating the velocity potential of bubble β.

In coordinates β, the velocity potential of bubble β is

$$\Phi_\beta(r_\beta,\theta_\beta,t)=\Phi_{\beta 0}(r_\beta,t)+\epsilon\Phi_{\beta 2}(r_\beta,\theta_\beta,t), \tag{10}$$

where

$$\Phi_{\beta 0}(r_\beta,t)=\frac{B_0(t)}{r_\beta}, \tag{11}$$

$$\Phi_{\beta 2}(r_\beta,\theta_\beta,t)=\frac{B_2(t)}{r_\beta^3}P_2(\cos\theta_\beta). \tag{12}$$

Here, $\Phi_{\beta 0}(r_\beta, t)$ and $\Phi_{\beta 2}(r_\beta, \theta_\beta, t)$ denote the spherical component and the nonspherical component of the velocity potential of bubble β. $B_0(t)$ and $B_2(t)$ are two functions of time. Equations (11) and (12) can be obtained from a study by Chen et al. [14].

To calculate the total velocity potential for a point in the liquid, we need to convert the expression of the velocity potential of bubble β from coordinates β to coordinates α. When r_α is near the interface of bubble α, namely $r_\alpha \ll L$, we have the following relations [15–19]:

$$\frac{1}{r_\beta}=\frac{1}{\sqrt{L^2-2Lr_\alpha\cos\theta_\alpha+r_\alpha^2}}=\frac{1/L}{\sqrt{1-2(r_\alpha/L)\cos\theta_\alpha+(r_\alpha/L)^2}}$$
$$=\sum_{i=0}^{\infty}\frac{r_\alpha^i}{L^{i+1}}P_i(\cos\theta_\alpha), \tag{13}$$

$$\frac{P_2(\cos\theta_\beta)}{r_\beta^3}=\frac{1}{L^3}\sum_{i=0}^{\infty}C_{2+i}^2\left(\frac{r_\alpha}{L}\right)^i P_i(\cos\theta_\alpha), \tag{14}$$

where

$$C_{2+i}^2=\frac{(2+i)!}{2!\,i!}=\frac{(i+2)(i+1)}{2},$$

and $P_i(\cos\theta_\alpha)$ is the ith-order Legendre function.

Substituting these relations into equations (11) and (12), we obtain the velocity potentials of bubble β in coordinates α:

$$\Phi_{\beta 0}(r_\alpha,t)=\frac{B_0(t)}{L}\sum_{i=0}^{\infty}\left(\frac{r_\alpha}{L}\right)^i P_i(\cos\theta_\alpha), \tag{15}$$

$$\Phi_{\beta 2}(r_\alpha,\theta_\alpha,t)=\frac{B_2(t)}{L^3}\sum_{i=0}^{\infty}C_{2+i}^2\left(\frac{r_\alpha}{L}\right)^i P_i(\cos\theta_\alpha). \tag{16}$$

In addition, according to the sphere theorem by Weiss [20], when bubble α exists in an arbitrary irrotational flow,

it can cause a disturbance to this flow. Thus, an extra perturbing velocity potential can occur in the vicinity of the interface of bubble α. When the flow is undisturbed by bubble α, the unperturbed velocity potential of the flow should be Φ_β. Hence, under the disturbance of bubble α, we denote the perturbing velocity potential as $\Phi_{\beta\to\alpha}(r_\alpha, \theta_\alpha, t)$, which is also the additional velocity potential induced by bubble β in the vicinity of the interface of bubble α.

The perturbing velocity potential can be calculated by the following equality [20]:

$$\Phi_{\beta\to\alpha}(r_\alpha,\theta_\alpha,t)=\frac{S_\alpha}{r_\alpha}\Phi_\beta\left(\frac{S_\alpha^2}{r_\alpha},\theta_\alpha,t\right)-\frac{2}{S_\alpha r_\alpha}\int_0^{S_\alpha}\lambda\Phi_\beta\left(\frac{\lambda^2}{r_\alpha},\theta_\alpha,t\right)d\lambda.$$

Substituting equations (15) and (16) into the above equality, we obtain

$$\Phi_{\beta\to\alpha}(r_\alpha,\theta_\alpha,t)=\frac{B_0(t)}{L}\sum_{i=0}^{\infty}\frac{i}{i+1}\frac{S_\alpha^{2i+1}}{r_\alpha^{i+1}L^i}P_i(\cos\theta_\alpha)$$
$$+\epsilon\frac{B_2(t)}{L^3}\sum_{j=0}^{\infty}C_{2+j}^2\frac{j}{j+1}\frac{S_\alpha^{2j+1}}{r_\alpha^{j+1}L^j}P_j(\cos\theta_\alpha). \tag{17}$$

Similarly, $\Phi_{\alpha\to\beta}(r_\alpha, \theta_\alpha, t)$ represents the perturbing velocity potential induced by bubble α in the vicinity of the interface of bubble β. However, we assume that $L \gg S_\alpha + S_\beta$. Thus, the effect of $\Phi_{\alpha\to\beta}(r_\alpha, \theta_\alpha, t)$ on the vicinity of the interface of bubble α is extremely small. By calculation, we can formulate $\Phi_{\alpha\to\beta}(r_\alpha, \theta_\alpha, t) = O(1/L^{10})$ in coordinates α. Hence, the term $\Phi_{\alpha\to\beta}(r_\alpha, \theta_\alpha, t)$ can be neglected for the calculation of the total velocity potential.

In addition, the total velocity potential $\Phi(r_\alpha, \theta_\alpha, t)$ should be consistent with the radius function of bubble α (see Eqs. (1a)) in form. Thus, in the nonspherical term of $\Phi(r_\alpha, \theta_\alpha, t)$, only the terms about the second-order Legendre function $P_2(\cos\theta_\alpha)$ can be retained. The expression for the total velocity potential is:

$$\Phi(r_\alpha,\theta_\alpha,t)=\Phi_\alpha(r_\alpha,\theta_\alpha,t)+\Phi_\beta(r_\alpha,\theta_\alpha,t)+\Phi_{\beta\to\alpha}(r_\alpha,\theta_\alpha,t)$$
$$\approx\frac{A_0(t)}{kr_\alpha}-\frac{\dot{A}_0(t)}{\omega}+\frac{B_0(t)}{L}$$
$$+\epsilon P_2(\cos\theta_\alpha)\left\{\frac{3A_2(t)}{k^3r_\alpha^3}+\frac{2A_2(t)}{kr_\alpha}+\frac{\dot{A}_2(t)}{\omega}+\frac{B_2(t)}{L^5}\left[6r_\alpha^2+\frac{4S_\alpha^5}{r_\alpha^3}\right]\right\}. \tag{18}$$

At the interface of bubble α, the total velocity potential satisfies the following two equations:

$$\left.\frac{\partial\Phi}{\partial r_\alpha}\right|_{r_\alpha=S_\alpha}=\frac{\mathrm{d}S_\alpha}{\mathrm{d}t}, \tag{19}$$

$$\left.\frac{\partial\Phi}{\partial t}\right|_{r_\alpha=S_\alpha}+\frac{1}{2}(\nabla\Phi)^2\Big|_{r_\alpha=S_\alpha}=-\frac{\Delta P}{\rho}, \tag{20}$$

where the expression of ΔP see equation (4). Equation (20) is obtained when the gravity of the liquid is negligible and the liquid flow is irrotational. Substituting equations (1a) and (18) into equations (19) and (20), using the Taylor series expansion of ϵ, and only retaining the first two order terms for ϵ, we obtain

$$\dot{a}_0(t)+\frac{1}{ka_0^2(t)}A_0(t)=0, \tag{21}$$

$$\dot{a}_2(t)-\frac{2a_2(t)}{ka_0^3(t)}A_0(t)+\left[\frac{9}{k^3a_0^4(t)}+\frac{2}{ka_0^2(t)}\right]A_2(t)=0, \tag{22}$$

$$\frac{\dot{A}_0(t)}{ka_0(t)}+\omega A_0(t)+\frac{1}{2}\dot{a}_0^2(t)+\frac{\dot{B}_0(t)}{L}=-\frac{\Delta P_1}{\rho}, \tag{23}$$

$$\frac{\left[3+2k^2a_0^2(t)\right]\dot{A}_2(t)}{k^3a_0^3(t)}-\omega A_2(t)-\frac{a_2(t)\dot{A}_0(t)}{ka_0^2(t)}+\dot{a}_0(t)\dot{a}_2(t)$$
$$+\frac{20a_0(t)\dot{a}_0(t)}{L^5}B_2(t)+\frac{10a_0^2(t)}{L^5}\dot{B}_2(t)=-\frac{f_\mathrm{e}}{\rho}. \tag{24}$$

At the interface of bubble β, the total velocity potential satisfies the following equation [20]:

$$\left.\frac{\partial\Phi}{\partial r_\beta}\right|_{r_\beta=S_\beta}=\left.\frac{\partial\Phi_\beta}{\partial r_\beta}\right|_{r_\beta=S_\beta}=\frac{\mathrm{d}S_\beta}{\mathrm{d}t}. \tag{25}$$

Substituting equations (1b) and (10)–(12) into equation (25), using the Taylor series expansion of ϵ, and neglecting the Peano remainder $O(\epsilon^2)$, we obtain

$$\dot{b}_0(t)+\frac{1}{b_0^2(t)}B_0(t)=0, \tag{26}$$

$$\dot{b}_2(t)-\frac{2b_2(t)}{b_0^3(t)}B_0(t)+\frac{3}{b_0^4(t)}B_2(t)=0. \tag{27}$$

Here, the liquid's compressibility is not considered.

Let $R_{\alpha 0}$ and $R_{\beta 0}$ be initial radii of bubble α and bubble β, namely $R_{\alpha 0} = a_0(0)$ and $R_{\beta 0} = b_0(0)$. After eliminating $A_0(t)$, $A_2(t)$, $B_0(t)$, $B_2(t)$, and their derivatives from the equations consisted by equations (21)–(24) and equations (26)–(27), we obtain the model for bubble α under the action of bubble β:

$$a_0(t)\ddot{a}_0(t)+\frac{3}{2}\dot{a}_0^2(t)+k\omega a_0^2(t)\dot{a}_0(t)+\frac{b_0(t)}{L}I_{b0}=\frac{\Delta P_1}{\rho}, \tag{28a}$$

$$\frac{N}{M}a_0(t)\ddot{a}_2(t)+Z_\beta\dot{a}_2(t)+Z_\varpi a_2(t)+\frac{20a_0(t)\dot{a}_0(t)}{3L^5}I_{b1}$$
$$+\frac{10a_0^2(t)b_0^2(t)}{3L^5}I_{b2}=\frac{f_\mathrm{e}}{\rho}, \tag{28b}$$

where

$$\begin{cases} k=\frac{\omega}{c} \\ M=9+2k^2a_0^2(t) \\ N=3+2k^2a_0^2(t) \\ Z_\beta=\left[\frac{6N-M}{M}-\frac{4k^2a_0^2(t)N}{M^2}\right]\dot{a}_0(t)-\frac{k^3\omega a_0^4(t)}{M} \\ Z_\varpi=\left(\frac{6N}{M}-2\right)\frac{\dot{a}_0^2(t)}{a_0(t)}+\left(\frac{2N}{M}-1\right)\ddot{a}_0(t) \\ \quad -\frac{8k^2a_0(t)\dot{a}_0^2(t)N}{M^2}-\frac{2k^3\omega a_0^3(t)\dot{a}_0(t)}{M} \\ I_{b0}=2\dot{b}_0^2(t)+b_0(t)\ddot{b}_0(t) \\ I_{b1}=b_0^3(t)\left[2\dot{b}_0(t)b_2(t)+b_0(t)\dot{b}_2(t)\right] \\ I_{b2}=6\dot{b}_0^2(t)b_2(t)+2b_0(t)\ddot{b}_0(t)b_2(t) \\ \quad +6b_0(t)\dot{b}_0(t)\dot{b}_2(t)+b_0^2(t)\ddot{b}_2(t) \\ \Delta P_1=\left(p_0+\frac{2\sigma}{R_{\alpha 0}}-p_\mathrm{v}\right)\left[\frac{R_{\alpha 0}}{a_0(t)}\right]^{3\gamma}+p_\mathrm{v}-p_0 \\ \quad -\frac{2\sigma}{a_0(t)}-\frac{4\eta\dot{a}_0(t)}{a_0(t)}-p_\mathrm{a}\cos\omega t \\ f_\mathrm{e}=\left\{1-\left[\frac{R_{\alpha 0}}{a_0(t)}\right]^{3\gamma}\right\}\epsilon_0\frac{(\epsilon_{\mathrm{r}1}-1)^2}{3}E^2. \end{cases}$$

Equation (28a) is a modified Rayleigh-Plesset equation for $a_0(t)$. The term $k\omega a_0^2(t)\dot{a}_0(t)$ is related to the oscillation resistance induced by the liquid's compressibility. Equation (28b) can be regarded as a damped vibration equation for $a_2(t)$ with external forces, without consideration of time-varying coefficients. In addition, all terms for L are related to the forces that bubble β exerts on bubble α.

Following similar steps, we can also obtain the model for bubble β under the action of bubble α, which has a similar form as the model for bubble α.

$$b_0(t)\ddot{b}_0(t)+\frac{3}{2}\dot{b}_0^2(t)+k\omega b_0^2(t)\dot{b}_0(t)+\frac{a_0(t)}{L}I_{a0}=\frac{\Delta P_1'}{\rho}, \quad (29a)$$

$$\frac{N'}{M'}b_0(t)\ddot{b}_2(t)+Z_\beta'\dot{b}_2(t)+Z_\varpi'b_2(t)+\frac{20b_0(t)\dot{b}_0(t)}{3L^5}I_{a1} +\frac{10b_0^2(t)a_0^2(t)}{3L^5}I_{a2}=\frac{f_\mathrm{e}'}{\rho}, \quad (29b)$$

where

$$\begin{cases} M'=9+2k^2b_0^2(t) \\ N'=3+2k^2b_0^2(t) \\ Z_\beta'=\left[\frac{6N'-M'}{M'}-\frac{4k^2b_0^2(t)N'}{(M')^2}\right]\dot{b}_0(t)-\frac{k^3\omega b_0^4(t)}{M'} \\ Z_\varpi'=\left(\frac{6N'}{M'}-2\right)\frac{\dot{b}_0^2(t)}{b_0(t)}+\left(\frac{2N'}{M'}-1\right)\ddot{b}_0(t) \\ \quad -\frac{8k^2b_0(t)\dot{b}_0^2(t)N'}{(M')^2}-\frac{2k^3\omega b_0^3(t)\dot{b}_0(t)}{M'} \\ I_{a0}=2\dot{a}_0^2(t)+a_0(t)\ddot{a}_0(t) \\ I_{a1}=a_0^3(t)[2\dot{a}_0(t)a_2(t)+a_0(t)\dot{a}_2(t)] \\ I_{a2}=6\dot{a}_0^2(t)a_2(t)+2a_0(t)\ddot{a}_0(t)a_2(t) \\ \quad +6a_0(t)\dot{a}_0(t)\dot{a}_2(t)+a_0^2(t)\ddot{a}_2(t) \\ \Delta P_1'=\left(p_0+\frac{2\sigma}{R_{\beta 0}}-p_\mathrm{v}\right)\left[\frac{R_{\beta 0}}{b_0(t)}\right]^{3\gamma}+p_\mathrm{v}-p_0 \\ \quad -\frac{2\sigma}{b_0(t)}-\frac{4\eta\dot{b}_0(t)}{b_0(t)}-p_\mathrm{a}\cos\omega t \\ f_\mathrm{e}'=\left\{1-\left[\frac{R_{\beta 0}}{b_0(t)}\right]^{3\gamma}\right\}\epsilon_0\frac{(\epsilon_{\mathrm{r}l}-1)^2}{3}E^2 \end{cases}.$$

When $c\to\infty$, namely $k\to 0$, equations (28a)–(28b) and equations (29a)–(29b) are reduced to the equations for an incompressible liquid,

$$a_0(t)\ddot{a}_0(t)+\frac{3}{2}\dot{a}_0^2(t)+\frac{b_0(t)}{L}I_{b0}=\frac{\Delta P_1}{\rho}, \quad (30a)$$

$$\frac{1}{3}a_0(t)\ddot{a}_2(t)+\dot{a}_0(t)\dot{a}_2(t)-\frac{1}{3}\ddot{a}_0(t)a_2(t)+\frac{20a_0(t)\dot{a}_0(t)}{3L^5}I_{b1} +\frac{10a_0^2(t)b_0^2(t)}{3L^5}I_{b2}=\frac{f_\mathrm{e}}{\rho}, \quad (30b)$$

$$b_0(t)\ddot{b}_0(t)+\frac{3}{2}\dot{b}_0^2(t)+\frac{a_0(t)}{L}I_{a0}=\frac{\Delta P_1'}{\rho}, \quad (31a)$$

$$\frac{1}{3}b_0(t)\ddot{b}_2(t)+\dot{b}_0(t)\dot{b}_2(t)-\frac{1}{3}\ddot{b}_0(t)b_2(t)+\frac{20b_0(t)\dot{b}_0(t)}{3L^5}I_{a1} +\frac{10b_0^2(t)a_0^2(t)}{3L^5}I_{a2}=\frac{f_\mathrm{e}'}{\rho}. \quad (31b)$$

When $L\to\infty$, equations (30a) and (30b) can be further reduced to the equations for a single nonspherical bubble, see equations (32a) and (32b).

$$a_0(t)\ddot{a}_0(t)+\frac{3}{2}\dot{a}_0^2(t)=\frac{\Delta P_1}{\rho}, \quad (32a)$$

$$\frac{1}{3}a_0(t)\ddot{a}_2(t)+\dot{a}_0(t)\dot{a}_2(t)-\frac{1}{3}\ddot{a}_0(t)a_2(t)=\frac{f_\mathrm{e}}{\rho}. \quad (32b)$$

3 Numerical solutions and analysis

3.1 Effect of the distance between bubble centers on the radius of bubble α

By solving equations (28a)–(28b) and equations (29a)–(29b) numerically, we obtain the temporal evolutions of the spherical coefficient $a_0(t)$ and the nonspherical coefficient $a_2(t)$ of bubble α at different distances between bubble centers (see Figs. 2 and 3). In these two figures, the condition $L\to\infty$ represents the oscillation of an isolated nonspherical bubble. The other parameters see Table 1.

In Figure 2, the variations of $a_0(t)$ with time, at different distances L, have a similar pattern. Within one period, $a_0(t)$ first increases rapidly to its maximum during the rarefaction cycle, then, it decreases sharply to its minimum in a rather short time. This is followed by a series of rebounds. Furthermore, as the distance between two bubbles increases, the maximum of $a_0(t)$ increases, and, correspondingly, the minimum of $a_0(t)$ decreases. When $L\to\infty$, $a_0(t)$ reaches its highest maximum and lowest minimum. In Figure 3, $a_2(t)$ shows exponential increases with time during the first period. Theoretically, $a_2(t)$ shows a larger increase at a longer distance L. In other words, when the distance between bubble centers is longer, bubble α is subject to

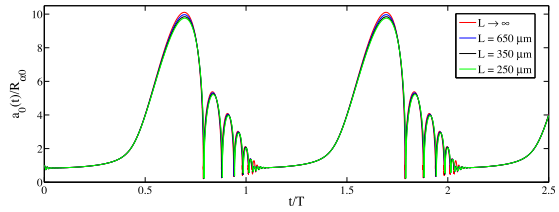

Figure 2. Temporal evolution of $a_0(t)$ at different distances between bubble centers (L) ($T = 50$ μs, $R_{\alpha 0} = 4.5$ μm).

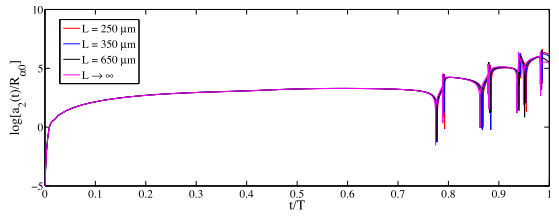

(a)

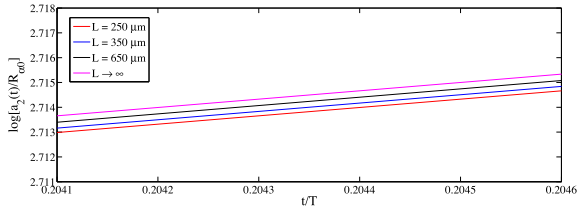

(b)

Figure 3. (a) Temporal evolution of $a_2(t)$ at different distances between bubble centers (L) ($T = 50$ μs, $R_{\alpha 0} = 4.5$ μm); (b) Partial enlarged detail of (a).

lower oscillation resistance from bubble β, and appears to be more ellipsoidal. The similar time-varying curves of $a_2(t)$ were also reported by Liang et al. [11, 21, 22] and Chen et al. [14].

3.2 Effect of the initial radius of bubble β on the radius of bubble α

When the distance is fixed at $L = 350$ μm, and the value of $R_{\beta 0}$ is variable, we can solve the equations (28a)–(28b) and equations (29a)–(29b) numerically and obtain time-varying curves of two radius components of bubble α. All parameters are the same as in Section 3.1. As depicted in Figure 4, when $R_{\beta 0} \leq 3.5$ μm, the wave peaks of $a_0(t)$ increase, while $R_{\beta 0}$ is increasing. However, as the initial radius $R_{\beta 0}$ increases from 3.5 μm to 6 μm, the wave peaks of $a_0(t)$ decrease significantly. Hence, the highest maximum and the lowest minimum of $a_0(t)$ occur when $R_{\beta 0} = 3.5$ μm. Moreover, the spherical component $a_0(t)$ undergoes faster oscillation damping for smaller $R_{\beta 0}$ values. Figure 5 reveals that, when bubble β has a higher initial radius $R_{\beta 0}$, the coefficient $a_2(t)$ shows a lower increase during one oscillation period. This means that the nonspherical feature of bubble α is more significant for smaller $R_{\beta 0}$ values.

Table 1. Simulation parameters.

Parameter	Value
Density of water, ρ	1000 kg m^{-3}
Adiabatic index, γ	1.4
Static pressure of water, p_0	1.013×10^5 Pa
Angular frequency of acoustic wave, ω	$2\pi \times 20 \times 10^3$ rad s^{-1}
Period of acoustic wave, T	50 μs
Viscosity of water, η	8.9×10^{-4} kg m^{-1} s^{-1}
Surface tension at the bubble wall, σ	7.6×10^{-2} N m^{-1}
Vapor pressure of water, p_v	2334.8 Pa
Acoustic pressure amplitude, p_a	1.35 p_0
Initial radius of bubble α, $R_{\alpha 0}$	4.5 μm
Initial radius of bubble β, $R_{\beta 0}$	4.5 μm
Speed of sound, c	1480 m s^{-1}
Electric field strength, E	2 MV m^{-1}
Vacuum permittivity, ε_0	8.854×10^{-12} F m^{-1}
Relative permittivity, ε_{rl}	78.3
$\dot{a}_0(0)$, $a_2(0)$, $\dot{a}_2(0)$	0
$\dot{b}_0(0), b_2(0), \dot{b}_2(0)$	0

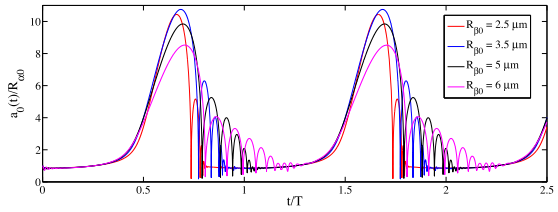

Figure 4. Temporal evolution of $a_0(t)$ for different initial radii of bubble β ($T = 50$ μs, $R_{\alpha 0} = 4.5$ μm).

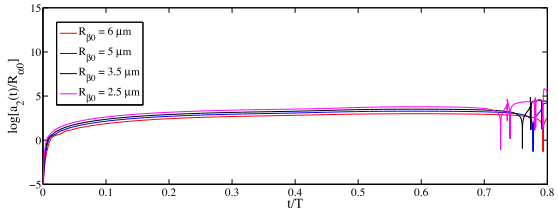

Figure 5. Temporal evolution of $a_2(t)$ for different initial radii of bubble β ($T = 50$ μs, $R_{\alpha 0} = 4.5$ μm).

3.3 Analyses of the cavitation of bubble α using approximate equations

These rapid increases of the coefficient $a_2(t)$, as shown in Figures 3 and 5, are unlikely to occur physically. In fact, it is impossible for $a_2(t)$ to increase without limits. This can be interpreted as follows: A nonspherical bubble has already collapsed before its nonspherical coefficient $a_2(t)$ reaches such a large value. The variation curves of $a_2(t)$ are only the results of the numerical solution to dynamic equations. Thus, to further investigate the effect of bubble β during the cavitation of bubble α, we introduce approximate equations. The method is to take the mean of electric stress f_s in half period, and approximately transform a nonspherical bubble into a spherical bubble. The reason for adopting this method is as follows: the presence of electric stress reduces

the surface tension at a bubble wall, which causes a bubble to expand more during the rarefaction cycle. Therefore, it is more suitable to take the mean of electric stress f_s in half period, rather than the mean of the bubble radius $S(\theta,\ t)$ in half period. A nonspherical bubble should be approximately treated as a spherical bubble with smaller surface tension, instead of a spherical bubble with a larger initial radius.

The mean of f_s in half period is

$$\overline{f_s} = \frac{2}{\pi}\int_0^{\frac{\pi}{2}} f_s \,\mathrm{d}\theta = \epsilon_0 \frac{(\epsilon_{rl}-1)^2}{12}E^2. \tag{33}$$

Let R_α and R_β be radii of approximate spherical bubbles of bubble α and bubble β. By inserting the term $\epsilon\overline{f_s}$ into the right sides of equations (28a) and (29a) and replacing $a_0(t)$ and $b_0(t)$ with R_α and R_β, we can rewrite equations (28a) and (29a) as

$$R_\alpha\ddot{R}_\alpha + \frac{3}{2}\dot{R}_\alpha^2 + k\omega R_\alpha^2\dot{R}_\alpha + \frac{R_\beta}{L}I_{R\beta} = \frac{\Delta P_M}{\rho}, \tag{34a}$$

$$R_\beta\ddot{R}_\beta + \frac{3}{2}\dot{R}_\beta^2 + k\omega R_\beta^2\dot{R}_\beta + \frac{R_\alpha}{L}I_{R\alpha} = \frac{\Delta P'_M}{\rho}, \tag{34b}$$

where

$$\begin{cases} I_{R\beta} = 2\dot{R}_\beta^2 + R_\beta\ddot{R}_\beta \\ I_{R\alpha} = 2\dot{R}_\alpha^2 + R_\alpha\ddot{R}_\alpha \\ \Delta P_M = \left(p_0 + \frac{2\sigma}{R_{\alpha 0}} - p_v - \epsilon\overline{f_s}\right)\left(\frac{R_{\alpha 0}}{R_\alpha}\right)^{3\gamma} + p_v \\ \qquad -p_0 - \frac{2\sigma}{R_\alpha} - \frac{4\eta\dot{R}_\alpha}{R_\alpha} + \epsilon\overline{f_s} - p_a\cos\omega t \\ \Delta P'_M = \left(p_0 + \frac{2\sigma}{R_{\beta 0}} - p_v - \epsilon\overline{f_s}\right)\left(\frac{R_{\beta 0}}{R_\beta}\right)^{3\gamma} + p_v \\ \qquad -p_0 - \frac{2\sigma}{R_\beta} - \frac{4\eta\dot{R}_\beta}{R_\beta} + \epsilon\overline{f_s} - p_a\cos\omega t. \end{cases}$$

The equations (34a) and (34b) are the approximate equations that describe the radius variations of bubble α and bubble β with the interaction between two bubbles. To simplify the calculation, we assume that $\epsilon = 0.1$ in the following analysis. As long as $\epsilon > 0$, all conclusions below do not change with the ϵ value.

3.3.1 Effect of bubble β on the radius of bubble α

In Section 3.2, we concluded that, when $R_{\beta 0} = 3.5$ μm, $a_0(t)$ reaches its highest maximum and lowest minimum. Thus, the numerical solutions of equations (34a) and (34b) are performed for the bubble pair with initial radii $R_{\alpha 0} = 4.5$ μm and $R_{\beta 0} = 3.5$ μm. All other parameters are the same as in Section 3.1. Figure 6 shows the temporal evolution of R_α at different distances between two bubbles. The condition $L \to \infty$ reflects the oscillation of an isolated bubble. With increasing distance between bubble centers, the oscillation amplitude of the radius of bubble α increases. This can be explained as follows: A longer distance between bubble centers leads to less oscillation resistance and higher

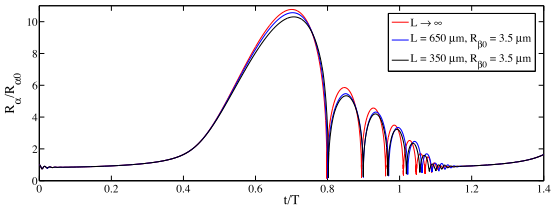

Figure 6. Temporal evolution of R_α at different distances between bubble centers (L) (T = 50 μs, $R_{\alpha 0}$ =4.5 μm).

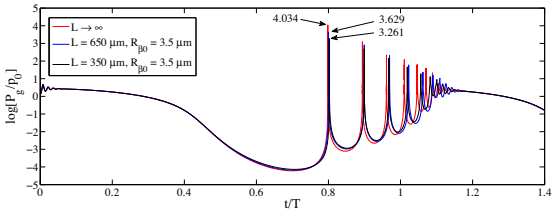

Figure 7. Temporal evolution of P_g at different distances between bubble centers (L) (T = 50 μs, $R_{\alpha 0}$ = 4.5 μm, p_0 = 1.013×10^5 Pa).

expansion during the rarefaction cycle for bubble α. During the compression cycle, bubble α with a larger maximum radius undergoes a more violent collapse, and it therefore reaches a lower minimum radius. Hence, the highest maximum radius and the lowest minimum radius are obtained during the oscillation of an isolated bubble.

3.3.2 Effect of bubble β on the gas pressure and the temperature inside bubble α

When the van der Waals hard-core radius h is taken into account, the expressions for the gas pressure P_g and the temperature T_g in the center of bubble α are given by [23, 24]

$$\begin{cases} P_g = \left(p_0 + \frac{2\sigma}{R_{\alpha 0}} - p_v - \epsilon\overline{f_s}\right)\left(\frac{R_{\alpha 0}^3 - h^3}{R_\alpha^3 - h^3}\right)^\gamma \\ T_g = T_0\left(\frac{R_{\alpha 0}^3 - h^3}{R_\alpha^3 - h^3}\right)^{\gamma-1}, \end{cases}$$

where T_0 is the ambient temperature, T_0 = 298.15 K. For bubble α with an initial radius $R_{\alpha 0}$ = 4.5 μm, $h = R_{\alpha 0}/8.54 \approx 0.53$ μm. As shown in Figures 7 and 8, under all conditions, the maximum gas-pressure and temperature inside bubble α occur at the end of the collapse, when bubble α reaches its minimum radius. Furthermore, during the negative pressure phase of the ultrasound wave, the maximum internal pressure and temperature of an isolated bubble are significantly higher, compared to a bubble with another adjacent bubble. In general, regardless of the distance between two bubbles and the initial radius of an adjacent bubble, the interaction between two bubbles always acts as resistance to the oscillation of a bubble, when parameters of ultrasound and an electrostatic field are constant.

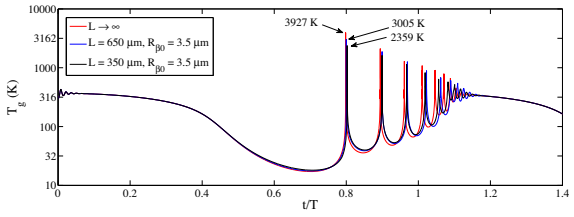

Figure 8. Temporal evolution of T_g at different distances between bubble centers (L) (T = 50 μs, $R_{\alpha 0}$ = 4.5 μm, T_0 = 298.15 K).

4 Conclusion

In the present study, we developed a model for two interacting nonspherical bubbles in a compressible liquid under the coupling effect of ultrasound and electrostatic field. When the distance between bubble centers is shorter, bubble α is subject to higher oscillation resistance from bubble β, and appears to be more ellipsoidal. When the initial radius $R_{\beta 0}$ equals to 3.5 μm, $a_0(t)$ reaches its highest maximum and lowest minimum. For a larger $R_{\beta 0}$ value, the nonspherical feature of bubble α becomes more significant after several periods. By solving approximate equations numerically, we found that, at the end of the collapse, the maximum pressure and temperature inside an isolated bubble are significantly higher than a bubble with an adjacent bubble. However, this obtained model can only depict the interaction between two adjacent bubbles. In fact, when a number of bubbles undergo ultrasonic cavitation simultaneously, the interaction between them can be more complicated. Therefore, a subject of our future research could be the oscillation of a nonspherical bubble cluster, as well as the effect of the interaction on the resonance frequency of the investigated bubble.

Acknowledgments

This research were supported by Provincial Major Project in Basic and Applied Research of Natural Science (Department of Education of Guangdong Province) (No.2017GKZDXM015), National Natural Science Foundation of China (No.11464002), Innovation Team Project of Colleges and Universities in Guangdong Province (Natural Science) (No.2020KCXTD054), Key Scientific Research Platform of Colleges and Universities (Department of Education of Guangdong Province) (No.2021GCZX017), Special Project in Key Fields of Universities in Guangdong Province (Science and Technology Services for Rural Revitalization) (No.2022ZDZX4118), and Youth Innovation Talent Project of Universities in Guangdong Province (No.2022KQNCX261).

Data Availability Statement

The research data associated with this article are included within the article.

References

1. K.-W. Jung, M.-J. Hwang, M.-J. Cha, K.-H. Ahn: Application and optimization of electric field-assisted ultrasonication for disintegration of waste activated sludge using response surface methodology with a Box-Behnken design. Ultrasonics Sonochemistry 22 (2015) 437–445.
2. R.-F. Yang, L.-L. Geng, H.-Q. Lu, X.-D. Fan: Ultrasound-synergized electrostatic field extraction of total flavonoids from hemerocallis citrina baroni. Ultrasonics Sonochemistry 34 (2017) 571–579.
3. J.-J. Deng, R.-F. Yang, H.-Q. Lu: Dynamics of nonspherical bubble in compressible liquid under the coupling effect of ultrasound and electrostatic field. Ultrasonics Sonochemistry 71 (2021).
4. F. Li, J. Cai, X. Huai, B. Liu: Interaction mechanism of double bubbles in hydrodynamic cavitation. Journal of Thermal Science 22, 3 (2013) 242–249.
5. Y. Pityuk, N. Gumerov, O. Abramova, I. Zarafutdinov, I. Akhatov: Numerical study of interaction of two deformable bubbles in an acoustic field. Journal of Applied Mechanics and Technical Physics 60, 4 (2019) 661–668.
6. C. Wang, J. Cheng: The velocity field around two interacting cavitation bubbles in an ultrasound field. Science China-Physics Mechanics & Astronomy 56 (2013) 1246–1252.
7. A. Dehane, S. Merouani: Impact of dissolved rare gases (ar, xe and he) on single-bubble sonochemistry in the presence of carbon tetrachloride. Chemical Papers 76, 5 (2022) 3011–3030.
8. A. Dehane, S. Merouani, O. Hamdaoui, M.H. Abdellattif, B.-H. Jeon, Y. Benguerba: A full mechanistic and kinetics analysis of carbon tetrachloride (ccl4) sono-conversion: Liquid temperature effect. Journal of Environmental Chemical Engineering 9, 6 (2021).
9. A. Dehane, S. Merouani, O. Hamdaoui, M. Ashokkumar: An alternative technique for determining the number density of acoustic cavitation bubbles in sonochemical reactors. Ultrasonics Sonochemistry 82 (2022) 105872.
10. A. Shima, T. Fujiwara: The behavior of two bubbles near a solid wall. Archive of Applied Mechanics 62, 1 (1992) 53–61.
11. J.-F. Liang, W.-Z. Chen, W.-H. Shao, S.-B. Qi: Aspherical oscillation of two interacting bubbles in an ultrasound field. Chinese Physics Letters 29, 7 (2012) 074701.
12. M.C. Zaghdoudi, M. Lallemand: Study of the behaviour of a bubble in an electric field: steady shape and local fluid motion. International Journal of Thermal Sciences 39, 1 (2000) 39–52.
13. J.R. Reitz, F.J. Milford, R.W. Christy: Foundations of Electromagnetic Theory (4th edn.). Addison-Wesley Publishing Company, 2008.
14. W.-J. Wang, W.-Z. Chen, M.-J. Lu, R.-J. Wei: Bubble oscillations driven by aspherical ultrasound in liquid. Journal of the Acoustical Society of America 114, 4 (2003) 1898–1904.
15. A.A. Doinikov: Translational motion of two interacting bubbles in a strong acoustic field. Physical Review E 64, 2 (2001) 026301.
16. A.A. Doinikov, A. Bouakaz: Theoretical model for coupled radial and translational motion of two bubbles at arbitrary separation distances. Physical Review E 92, 4 (2015) 043001.
17. D.A. Varshalovich, A.N. Moskalev, V.K. Khersonsky: The quantum theory of angular momentum. World Scientific Publishing Co., Pte. Ltd., 1988.
18. M.L. Boas: Mathematical methods in the physical sciences (2nd edn.). John Wiley & Sons Inc., 1983.
19. K.F. Riley, M.P. Hobson, S.J. Bence: Mathematical methods for physics and engineering: a comprehensive guide (3rd edn.). Cambridge University Press, 2006.

20. P. Weiss: On hydrodynamical images. arbitrary irrotational flow disturbed by a sphere. Mathematical Proceedings of the Cambridge Philosophical Society 40, 3 (1944) 259–261.
21. J.-F. Liang, X. Wang, J. Yang, L. Gong: Dynamics of two interacting bubbles in a nonspherical ultrasound field. Ultrasonics 75 (2017) 58–62.
22. J.-F. Liang, X. Wu, Y. Qiao: Dynamics of twin bubbles formed by ultrasonic cavitation in a liquid. Ultrasonics Sonochemistry 80 (2021) 105837.
23. T. Hongray, B. Ashok, J. Balakrishnan: Oscillatory dynamics of a charged microbubble under ultrasound. Pramana 84, 4 (2015) 517–541.
24. M.P. Brenner, S. Hilgenfeldt, D. Lohse: Single-bubble sonoluminescence. Reviews of Modern Physics 74 (2002) 425–484.

Cite this article as: Deng J-J. Yu M. & Yang R-F. 2022. Interaction between double nonspherical bubbles in compressible liquid under the coupling effect of ultrasound and electrostatic field. Acta Acustica, **6**, 52.